

## Simulation of Disperse Lennard-Jones Polymer Chains

Jacob Horne  
11 November 2019

### Abstract

MD simulations of Lennard-Jones (LJ) polymer chains of various degrees of polymerization (DP) were used to investigate the effects of system size and dispersity in DP on the self-diffusion coefficients,  $D$ , and radii of gyration,  $R_g$ . Simulations of systems with varying numbers of chains revealed that the value and error of the estimated self-diffusion coefficients are relatively insensitive to both dispersity and system size. Furthermore, the presence of dispersity did not significantly influence the scaling behavior of  $D$  or  $R_g$  with the system DP. In contrast, the full distributions of  $R_g$  values were broadened substantially across various DPs by the inclusion of dispersity. Overall, these results indicate that the effects of dispersity are mitigated in quantities such as diffusion coefficients that represent averages over many constituent atoms.

### Motivation and Background

#### Why Disperse Chains?

It is well known that many key properties of polymeric systems, such as self-diffusion coefficients and radii of gyration, vary strongly with the degree of polymerization (DP) or molecular weight of the constituent chains. Accordingly, most simple first-principles models of bulk polymer behavior consider systems of identical chains with a precise DP or molecular weight. Unfortunately, this idealized system is often not realizable in practice. Nearly all synthetic polymers are disperse. This means that, while the *average* DP of a synthetic polymer mixture may be well controlled, typically by means of stoichiometry, the exact DPs of all constituent chains are distributed.

The effects of this distribution on molecular weight dependent properties is often difficult to intuit. While some properties depend primarily on the average DP, others may be strongly affected by exact shape of the distribution. Advances in synthetic techniques over the past few decades have popularized controlled polymerizations which produce relatively narrow and symmetric DP distributions.

Accordingly, it is worthwhile to investigate the potential effects of moderate dispersity, as would be expected in a synthetic polymer melt, on key system properties. In this case, systems of Lennard-Jones polymer chains with harmonic bonds are used to investigate the effects of dispersity in DP on the calculated self-diffusion coefficients and radii of gyration.

### Theoretical Background

Typically, the DP distribution of synthetic polymers is quantified by three metrics: the number average DP ( $N_n$ ), the weight average DP ( $N_w$ ), and the dispersity ( $\mathfrak{D} = N_w/N_n$ ). Statistical arguments can be used to derive an expression for the variance in terms of these three metrics; namely, Equation 1, below.

$$\sigma^2 = N_n^2(\mathfrak{D} - 1) \quad (1)$$

Traditional uncontrolled synthetic techniques such as free radical polymerization tend to produce broad DP distributions with large dispersities,  $\mathfrak{D} > 1.5$ . This characteristic broadness is generally a result of two main issues that arise during synthetic polymerizations: irreversible termination reactions and slow initiation relative to propagation rates. Synthetic techniques such as anionic polymerization have allowed for the mitigation of these issues and given rise to a host of controlled polymerization methods.

The DP distributions produced by these techniques are described well by a kinetic model known as the ideal living polymerization, which assumes the absence of termination reactions and simultaneous initiation of all growing chains. For such a system, the distribution of DPs is given by a modified Poisson distribution, shown in Equation 2.

$$p(N) = \frac{(N_n - 1)^{N-1} e^{-(N_n-1)}}{N - 1} \quad (2)$$

## Simulation Methodology

All systems considered in this study were comprised of  $N_c$  polymer chains with individual lengths  $M_i$  confined to a cubic box with side length  $L$  using periodic boundary conditions. The size of the box is related to the total number of atoms in the simulation box by the system average number density,  $\rho = N/L^3 = 0.8$ . The total number of atoms is calculated as the sum of all  $M_i$  in the system. A 2-D schematic of this system is depicted in Figure 1.

A pairwise force field was used to simulate interatomic energies and forces for all atoms in the system. The model, shown below in Equation 3, assumes Lennard-Jones type interactions for all non-bonded interactions and isotropic harmonic potentials for bonded atoms.

$$u_{ij} = \begin{cases} 4(r_{ij}^{-12} - r_{ij}^{-6}) & ij \text{ bonded} \\ \frac{k}{2}(r_{ij} - r_0)^2 & ij \text{ not bonded} \end{cases} \quad (3)$$

Here,  $k = 3000$  and  $r_0 = 1$  are the force constant and equilibrium bond distance that govern bonded interactions. For convenience of simulation and generality of results, all variables shown have been nondimensionalized using the length and energy scales of  $\sigma$  and  $\epsilon$  that appear in the typical Lennard-Jones potential.

Initial positions for each simulation were obtained by placing atoms on a cubic lattice and performing a local energy minimization using the conjugate gradient method. System temperature,  $T = 1$ , was controlled during equilibration by rescaling system velocities every 50 timesteps such that the total system kinetic energy  $E_k = 1.5T$ . Initial velocities were sampled randomly on the interval  $[0,1]$  for each atom, then rescaled to match the target system temperature. Timesteps were performed using the velocity Verlet algorithm with constant step size  $dt = 0.001$ .

All simulations detailed below were conducted in duplicate for both precise systems, with all chains of identical length (i.e.,  $M_i = M$  for all  $i$ ) and disperse systems, with  $M_i$  sampled randomly from the Poisson distribution given in Equation 2 with  $N = M_i$  and  $N_n = M$ . Data were obtained over production runs of  $t_{\text{prod}} = 100$  following two equilibration runs of  $t_{\text{equil}} = 10$  with velocity rescaling every 50 steps. During the second equilibration run, the total system energy was averaged and, before starting data production, system velocities were rescaled such that the current total system energy is exactly equal to the average value. Error bars, where shown, were obtained from replicate runs with different random number seeds under identical simulation conditions.

## Results and Discussion

### System Size Effects

To investigate the effects of varying system size, the mean-squared displacement (MSD) was tracked as a function of time for systems with varying  $M$  and  $N_c$ . Self-diffusion coefficients were then estimated for each system via linear regression as  $1/6$  of the slopes of these MSD curves. This process was repeated in triplicate and the standard deviations, referred to here as errors, of the resulting diffusion coefficients are shown Figure 2.

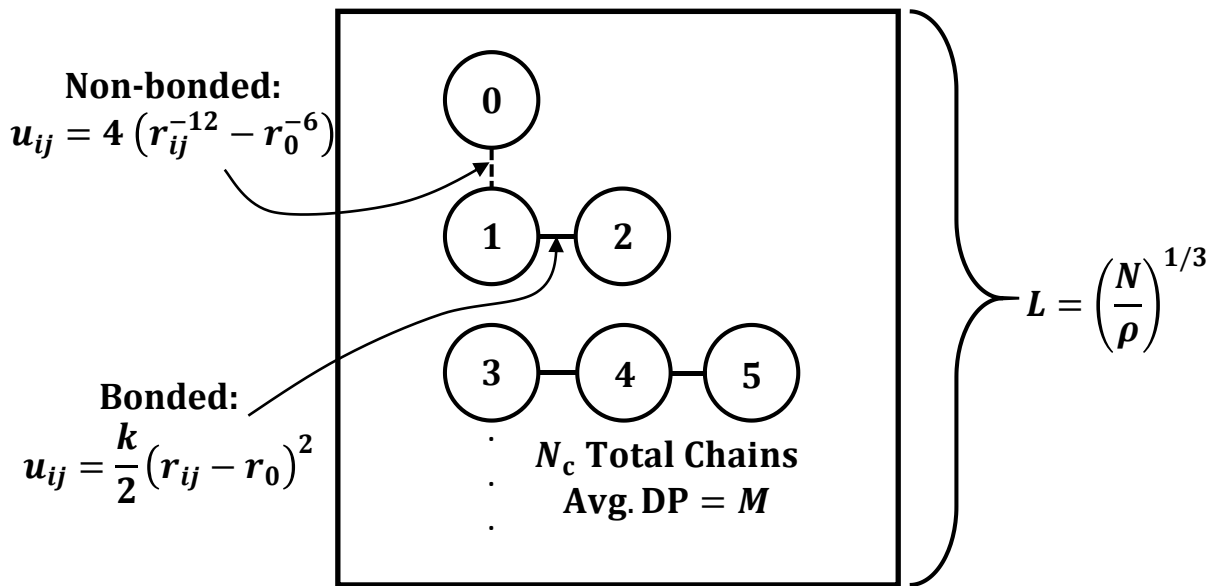


**Figure 1:** 2-D schematic rendering of disperse Lennard-Jones polymer chain system.

The error in the diffusion coefficients seems relatively insensitive to the total number of chains for systems of both precise and disperse chains. Although the errors for precise and disperse systems are nearly identical in most cases, there are a few interesting discrepancies. Systems of precise chains consistently exhibit an increase in the error at low  $N_c$  that is not obviously present in the disperse systems. This is likely a result of the random sampling for disperse systems which produces a significant population of higher molecular weight chains inflating the overall particle number and avoiding the trends associated with small system sizes. Although both precise and disperse systems exhibit a spike in the error over the range  $N_c \approx 25$  to 35, this feature is much more pronounced in the disperse systems, as seen in Figure 2b. The exact cause of this is unknown; however, it is worth noting that these problematic values of  $N_c$  also give uncharacteristically small diffusion coefficients.

### Self-Diffusion Coefficients

Based on analysis of the error in estimated self-diffusion coefficients at various system sizes, the diffusion coefficients were computed for systems of  $N_c = 20$  chains. Figure 3 shows these estimated diffusion coefficients on log-log axes for various values of  $M$  from 2 to 10. Intuitively, the diffusion coefficient is smaller for systems with longer chains. Qualitatively, the trends and values for precise and disperse systems are very similar. For each value of  $M$ , the precise and disperse diffusion coefficients differ by significantly less than the error in either.

Given that both trends are roughly linear on log-log axes, linear regression was used to roughly estimate the scaling of  $D$  with  $M$ . In this case, systems with precise chains appear to exhibit slightly stronger scaling with molecular weight,  $D_{\text{precise}} \sim M^{-0.5}$ , while  $D_{\text{disperse}} \sim M^{-0.4}$ . It is possible that this difference in scaling is a result of dispersity creating some degree of uniformity in systems with different  $M$  by including larger or smaller chains. However, given the modest difference in the estimated scaling, small number of data points, and large errors, this difference should not be overinterpreted.

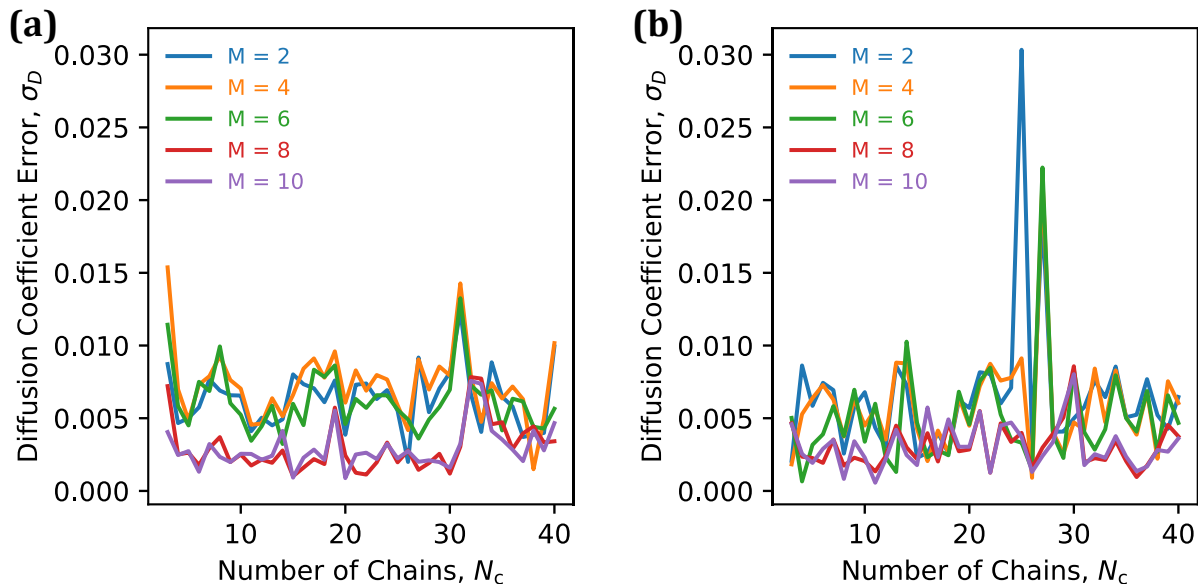


**Figure 2:** Error in calculated self-diffusion coefficients of (a) precise and (b) disperse polymer systems with varying numbers of simulated chains at various degrees of polymerization.

### Radius of Gyration

To visualize the effects of dispersity on system structural parameters, the distribution of  $R_g$  values was computed for systems of  $N_c = 20$  chains at various degrees of polymerization. Representative distributions are shown in Figures 3a, 3b, and 3c. In all cases, the presence of dispersity serves to broaden the distributions in  $R_g$ . Interestingly, this broadening seems to preserve the presence of any local features such as shoulders or local minima in the distribution. For precise systems with chain lengths  $M = 2$  and 5, the distribution of  $R_g$  is extremely narrow. The exact cause of this is unknown; however, varying the number of chains simulated had a strong effect on the shape of these

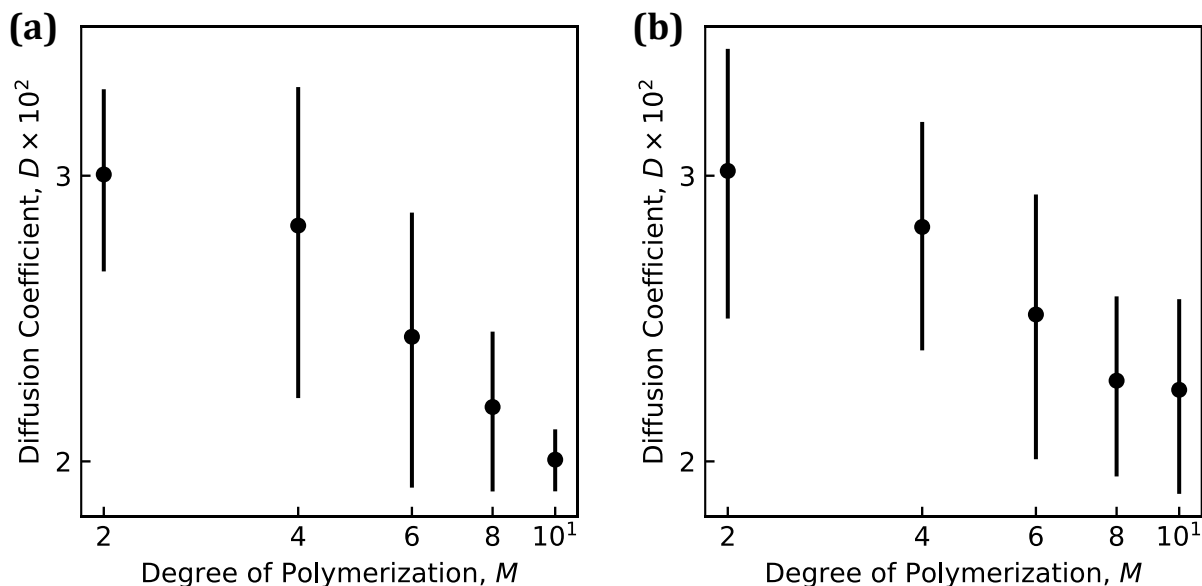


**Figure 3:** Calculated self-diffusion coefficients of (a) precise and (b) disperse polymer systems with  $N_c =$  varying at various degrees of polymerization, shown on log-log axes.

distributions, indicating that these extremely peaked distributions may be an artifact of the finite and small system size.

Figure 3d shows the variation of  $\langle R_g^2 \rangle^{1/2}$  with  $M$ . As expected,  $R_g$  increases with the degree of polymerization for both precise and disperse systems. As with the diffusion coefficients, the trends agree very well between precise and disperse systems. Disperse systems appear distributed slightly around the trend obeyed by precise systems; this is expected given the distribution of chains in each disperse system. Oddly, the values of  $M$  which gave uncharacteristically narrow distributions also produced values of  $R_g$  approximately half of that expected based on the trend from the other data. Although traditional polymer physics arguments suggest the scaling  $\langle R_g^2 \rangle^{1/2} \sim M^{1/2}$ , the trend in Figure 3d appears visually linear. This is likely an artifact of the small range of  $M$  values investigated.

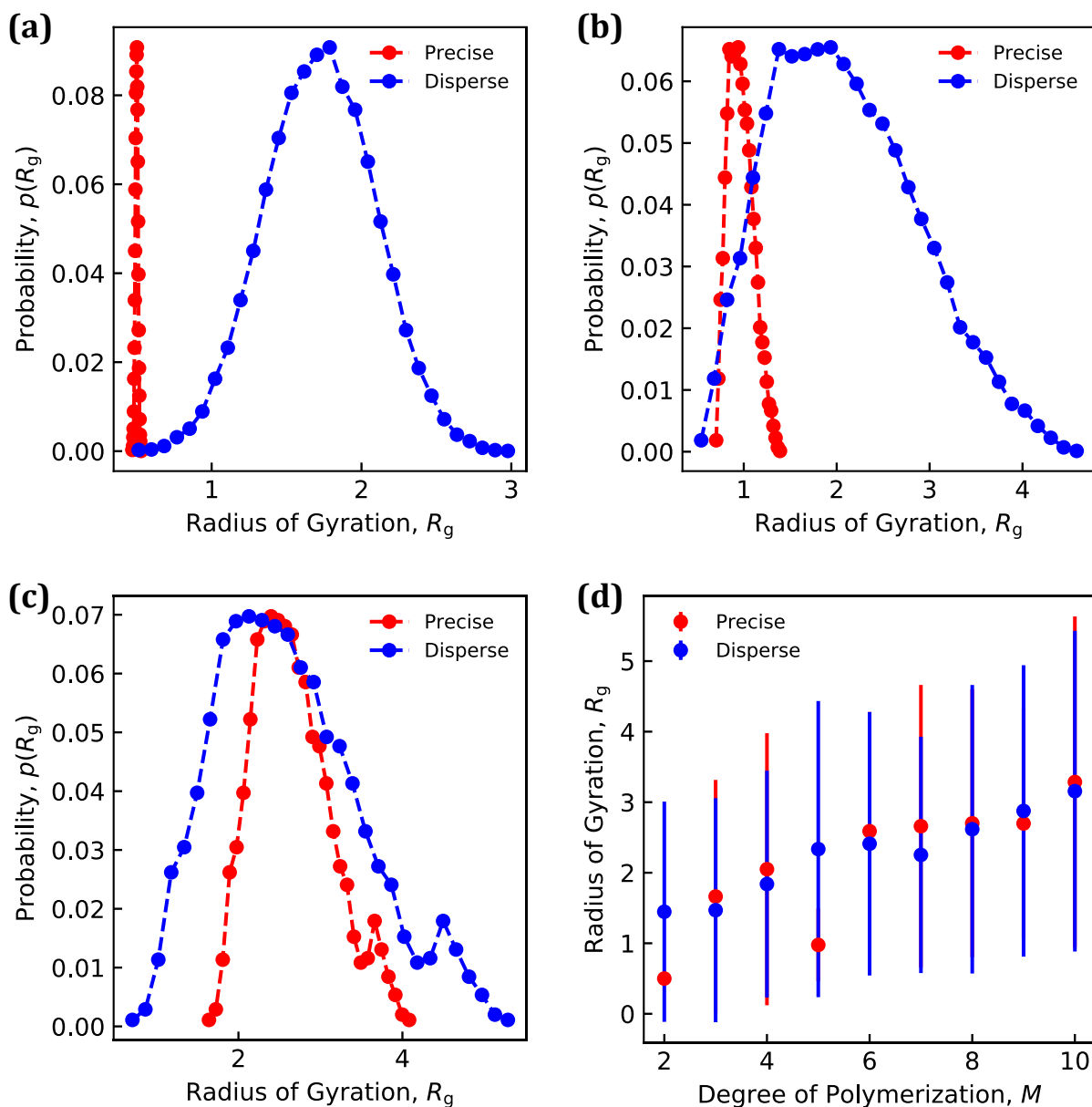


**Figure 4:** (a), (b), (c) Distribution of the radius of gyration,  $R_g$ , for  $M = 2, 5, 9$  and (d) variation in root mean squared  $R_g$  with degree of polymerization for  $M < 10$ .

**Movie Caption**

The movie provides a visualization of diffusion in a disperse melt of Lennard-Jones polymers with an average chain length of 10. A single chain of each length is uniquely colored to easily visualize the relative diffusion rates of different length chains.